

X-ray diffraction study of metallic VO₂

D. B. McWhan*

Bell Laboratories, Murray Hill, New Jersey 07974

M. Marezio†

Laboratoire de Rayons X, Centre National de la Recherche Scientifique B.P. 166 38042, Grenoble, France

J. P. Remeika and P. D. Dernier

Bell Laboratories, Murray Hill, New Jersey 07974

(Received 4 December 1973)

Refinement of the crystal structure of VO₂ at 360 and 470 K in the metallic rutile phase shows that both the vanadium and oxygen thermal displacements are larger than those found in rutile phases of TiO₂ and CrO₂ or monoclinic phases of VO₂ or V_{0.976}Cr_{0.024}O₂. The vanadium-vanadium distance along the rutile *c* axis is anomalously short when compared with neighboring rutile phases while the other nearest-neighbor metal-metal and metal-oxygen distances vary smoothly across the series. A comparison of Debye temperatures calculated from heat-capacity and x-ray data suggests the presence of low-lying vibrational modes in metallic VO₂.

INTRODUCTION

The driving force behind the metal-insulator transition in VO₂ has not been clearly established. Recent theoretical models for the transition are based on either strong electron-electron correlations¹⁻³ or changes in band structure⁴ which result from lattice softening.^{5,6} Experimentally, the large relatively-temperature-independent magnetic susceptibility of VO₂ and the large linear contribution to the heat capacity of the metallic phase of several vanadium oxides favor the former models.⁷ In x-ray studies of V_{0.976}Cr_{0.024}O₂ anomalously large Debye-Waller factors were found in the metallic rutile phase and this might be evidence for a lattice softening.⁸ In order to eliminate any possible effects resulting from the addition of chromium and in order to obtain accurate interatomic distances for the metallic phase of pure VO₂, the structure has been refined at 360 and 470 K. Large Debye-Waller factors have been found in agreement with the earlier studies on the rutile phase of V_{0.976}Cr_{0.024}O₂ and they are interpreted as evidence for possible soft modes in the metallic phase. Although the structure of the insulating phases of VO₂ and V_{0.976}Cr_{0.024}O₂ are quite different, both have reduced reciprocal-cell vectors corresponding to the ($\frac{1}{2}0\frac{1}{2}$) point in the unit cell of the metallic rutile phase and they might be interpreted as possible distortions resulting from a soft zone-edge mode in the metallic phase.

EXPERIMENTAL

Crystals of VO₂ were prepared by electrolysis of molten V₂O₅ containing vanadium metal. About 40.0 g of V₂O₅ were melted in a 100-cm³ platinum crucible. Granular V metal (2.0 g) was added to the melt. The platinum crucible served as anode

and a 1.5-mm-diam platinum wire was the cathode. The entire system was held at 800 °C in an argon atmosphere. Electrolysis was carried out at ~50 mA for 16 h. The resulting cluster of crystals on the cathode was washed in NH₄OH. The crystals were elongated prisms with well-developed faces and the largest were approximately 4×1×1 mm. The crystals were characterized by x-ray diffraction and electrical-resistivity measurements. The latter showed a change of 10⁵ at the metal-insulator transition which compares favorably with the best values reported in the literature.⁴ Some of the crystals of VO₂ were crushed into a fine powder and mixed with some finely divided silicon powder. This mixture was mounted on the platinum-resistance strip heater of a water-cooled high-temperature attachment for a Phillips-Norelco powder diffractometer. A complete 2θ scan was taken with Cu Kα radiation to check for possible extra phases. For each of five elevated temperatures where the rutile phase is stable, nine VO₂ reflections and four Si reflections in the angular range 70° < 2θ < 143° were recorded at a scanning rate of $\frac{1}{4}$ ° min⁻¹. A least-squares refinement gave the lattice parameters listed in Table I.

A crystal of VO₂ was ground into a sphere of radius 0.011 cm and was oriented by the precession method so that the rutile *b* axis would be coincident with the φ axis of the goniostat. X-ray intensity measurements were taken semiautomatically with a paper-tape-controlled General Electric XRD-5 diffractometer equipped with a scintillation counter and decade-scaler detection system. Zr-filtered Mo radiation was used with the diffractometer set at an 8° take-off angle. The integrated intensities were obtained by using the stationary-crystal stationary-counter technique where the background

TABLE I. Lattice parameters of the rutile phase of VO₂ at different temperatures.

T(K)	$a_R(\text{\AA})$	$c_R(\text{\AA})$
360	4.5546(3)	2.8514(2)
413	4.5555(4)	2.8552(3)
473	4.5561(5)	2.8598(3)
523	4.5573(5)	2.8626(3)
573	4.5580(4)	2.8663(2)

was measured at $\pm 2^\circ$ of 2θ off the peak maximum. Data were collected at 360 and 470 K. The sample temperature was maintained by blowing a hot stream of nitrogen gas directly on the crystal. A Varian temperature controller was used to monitor and regulate the gas flow and heater current. Reflections, which were known from the refinement of V_{0.976}Cr_{0.024}O₂ at 360 K to have nonzero intensity, were collected in the region $\chi \leq 45^\circ$ and $25^\circ < 2\theta < 80^\circ$. For each reflection the approximate angles φ , χ , and 2θ were set automatically and tuned manually. A φ scan was performed on each reflection in order to test whether the individual twins had coalesced in the rutile phase for that particular region of reciprocal space. These conditions resulted in 69 independent reflections which were used in the structural refinements.

The starting positional and thermal parameters were those obtained for the rutile phase of V_{0.976}Cr_{0.024}O₂ at 360 K. The scattering factors for neutral vanadium and oxygen atoms given by Cromer and Waber⁹ were used along with the real and imaginary components of the anomalous dispersion correction reported by Cromer.¹⁰ Complete convergence was obtained for each temperature after four cycles of refinement. The conventional R and wR factors were 0.017 and 0.025 at 360 K, and 0.016 and 0.024 at 470 K, respectively. The final positional and thermal parameters are reported in Table II; while the interatomic distances, bond angles, rms thermal displacements, and orientations are given in Tables III and IV.

DISCUSSION

The usual evidence for vanadium-vanadium interactions in VO₂ is the displacement of the vanadium atoms below the transition to form pairs along the pseudorutile c axis. However, even in the metallic rutile phase where the vanadium atoms are equally spaced along the c axis the average separation is shorter than in neighboring rutile phases. This distance also shows a larger variation with temperature (see Table I) with the coefficient of thermal expansion parallel to the c axis being five times greater than that perpendicular to c .¹¹ In Fig. 1 the metal-metal and metal-oxygen distances for TiO₂,¹² VO₂, CrO₂,¹³ and MnO₂¹⁴ are compared.

TABLE II. Positional and thermal parameters of VO₂ at 360 and 470 °K.

	360 K		470 K	
	V	O	V	O
x	0, 0	0, 3001(2)	0, 0	0, 3003(2)
y	0, 0	0, 3001(2)	0, 0	0, 3003(2)
z	0, 0	0, 0	0, 0	0, 0
β_{11}	0, 0106(2)	0, 0082(2)	0, 0121(2)	0, 0097(3)
β_{22}	0, 0106(2)	0, 0082(2)	0, 0121(2)	0, 0097(3)
β_{33}	0, 0233(7)	0, 015(1)	0, 0259(6)	0, 019(1)
β_{12}	0, 00108(8)	-0, 0018(3)	0, 00110(8)	-0, 0027(3)
β_{13}	0, 0	0, 0	0, 0	0, 0
β_{23}	0, 0	0, 0	0, 0	0, 0

The values for the rutile phase of VO₂ were obtained by extrapolating the high-temperature data to 298 K. In the rutile structure (space group $P4_2/mnm$) the metal-metal interatomic distances are determined by the lattice parameters as the vanadium atoms are at (0, 0, 0) and $(\frac{1}{2}, \frac{1}{2}, \frac{1}{2})$, but the oxygen atoms and hence the metal-oxygen distances depend on the positional parameter given in Table II. The positional parameter of the oxygen determined in the present study and in Ref. 8 is smaller than that determined earlier ($x = 0, 3000 \pm 2$ instead of $0, 305 \pm 3$).¹⁵ Thus, the difference between the equatorial and apical metal-oxygen distances is much smaller than that reported earlier. In Fig. 1 there is a smooth variation of both metal-oxygen distances and also the metal-metal distance across the shared corner of adjacent oxygen octahedra. However, the V-V distance across the shared edge of the oxygen octahedra is 0.09 Å shorter than expected from a smooth interpolation of the other data. (It follows that some of the V-O-V angles will also be anomalous). As suggested by Goodenough,⁶ it is reasonable to attribute this short distance in a molecular-orbital picture to additional binding caused by the d electrons either through direct overlap of d orbitals of adjacent vanadium atoms or via the oxygen atoms on the shared edge of adjacent oxygen octahedra. A calculation based on this model has been reported by Hearn.¹⁶ Recent augmented-plane-wave (APW)

TABLE III. Interatomic distances and angles in VO₂ at 360 and 470 °K.

	360 K	470 K
V-O × 2	1, 933(1) Å	1, 935(1) Å
V-O × 4	1, 921(1)	1, 924(1)
O-O × 2	2, 851(1)	2, 860(1)
O-O × 2	2, 575(1)	2, 573(1)
O-O × 8	2, 725(1)	2, 729(1)
O-V-O × 2	84, 17(6)°	83, 96(6)°
O-V-O × 2	95, 83(6)	96, 04(6)
O-V-O × 8	90, 00	90, 00
V-V across edge	2, 851(1) Å	2, 860(1) Å
V-V across corner	3, 522(1)	3, 525(1)

TABLE IV. rms components of thermal displacement ellipsoids of VO_2 at 360 K and 470 K and their orientation relative to the unit cell.

	360 K		470 K	
	V	O	V	O
r_1	0.098(1)	0.078(4)	0.104(1)	0.086(2)
r_2	0.100(1)	0.082(3)	0.108(1)	0.088(3)
r_3	0.111(1)	0.102(2)	0.118(1)	0.114(2)
r_1				
x	90	90	90	135
y	90	90	90	135
z	180	180	180	90
r_2				
x	45	45	45	90
y	135	45	135	90
z	90.0	90	90.0	0
r_3				
x	135	135	135	135
y	135	45	135	45
z	90.0	90	90.0	90

calculations of both phases of VO_2 suggest that covalent bonding is less important than implied in the molecular-orbital picture but that the conduction bands are sensitive functions of the dd and pd parameters.¹⁷

Although the c axis of VO_2 is shorter than expected, the thermal parameters of both the vanadium and oxygen atoms are larger than expected. In an anisotropic least-squares refinement the effect of the thermal displacements of each atom in the unit cell on the structure factor of a reflection with indices hkl is taken to have the form

$$\exp[-(\beta_{11}h^2 + \beta_{22}k^2 + \beta_{33}l^2 + 2\beta_{12}hk + 2\beta_{13}hl + 2\beta_{23}kl)],$$

where the values of β_{ij} allowed by symmetry are listed in Table II. The tensors are then reduced to give a thermal ellipsoid of the form

$$\exp[-8\pi^2\lambda^{-2}\sin\theta(\bar{u}_1^2l_1^2 + \bar{u}_2^2l_2^2 + \bar{u}_3^2l_3^2)],$$

where u_i and l_i are, respectively, the thermal displacements and the direction cosines of the i th axis of the ellipsoids relative to the scattering vector (Table IV). In Table V the thermal displacements of TiO_2 ,¹² VO_2 (rutile), $\text{V}_{0.976}\text{Cr}_{0.024}\text{O}_2$, (M_2)⁸ and CrO_2 (rutile)¹³ are compared. It is clear that the values for VO_2 are larger than for the other phases. The orientations of the thermal ellipsoids are not the same but the clear difference in their volume is evident. Only an isotropic refinement of the monoclinic phase of pure VO_2 has been reported¹⁸ but again the volume of the ellipsoids is comparable to those of the insulating phase of $\text{V}_{0.976}\text{Cr}_{0.024}\text{O}_2$ ⁸ and metallic CrO_2 .

In a band-theory model for the transition the large thermal displacements in the rutile phase would be interpreted as evidence for a lattice softening. A symmetry analysis of the rutile to monoclinic transition in pure VO_2 shows that a phonon instability at the zone edge ($\frac{1}{2}0\frac{1}{2}$) would be compatible with the observed change in symmetry.¹⁹ The addition of a small amount of CrO_2 (~1 mole%) to VO_2 leads to a markedly different distortion (M_2) from the rutile structure at the metal-insulator transition.⁸ However, the vectors of the reduced cell are compatible with the same phonon instability. The reduced cell of this phase is related to that of rutile by the matrix $[(1, 0, \bar{1})/(1, 0, 1)/(0, \bar{1}, 0)]$. This cell for $\text{V}_{0.976}\text{Cr}_{0.024}\text{O}_2$ at 298 K is

$$a_P = b_P = 5.3806 \text{ \AA} = \frac{1}{2}(a_c^2 + b_c^2)^{1/2},$$

$$c_P = 4.5255 \text{ \AA} = c_c,$$

$$\alpha_P = \beta_P = 91.58^\circ = 90^\circ + \arcsin \frac{a_c \sin(\beta_c - 90^\circ)}{2a_P},$$

$$\gamma_P = 65.19^\circ = 2 \arctan a_c / c_c.$$

It is a triclinic cell but because of the monoclinic symmetry it is given by four parameters. The reciprocal-lattice vectors of the reduced cell of this phase are compared with those of the insulating phase (M_1) of pure VO_2 and the first Brillouin zone of the rutile phase in Fig. 2. (The small changes in axis and interaxial angles at the transition have been neglected.) The same degenerate points occur for both monoclinic phases, namely ($\frac{1}{2}0\frac{1}{2}$) or the R point. A detailed group-theoretical analysis of the M_2 phase has shown that it is com-

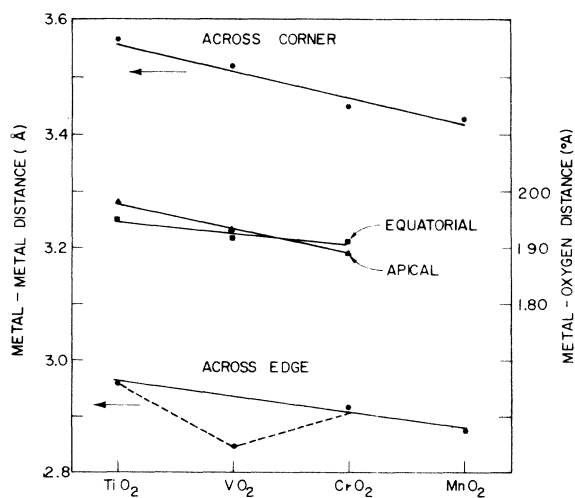


FIG. 1. Comparison of interatomic distances at 298 K in 3d transition metal oxides with the rutile structure showing the anomalously short vanadium-vanadium distance across the common edge of adjacent oxygen octahedra along the c axis.

TABLE V. Comparison of rms components of thermal displacement ellipsoids at 298 K.

MO ₂	M				O			
	u ₁ (Å)	u ₂ (Å)	u ₃ (Å)	V(Å ³)	u ₁ (Å)	u ₂ (Å)	u ₃ (Å)	V(Å ³)
TiO ₂ rutile	0.064(1)	0.079(1)	0.081(1)	0.0017(1)	0.053(2)	0.060(2)	0.085(1)	0.0011(1)
VO ₂ rutile	0.095(1)	0.095(1)	0.107(1)	0.0041(1)	0.073(3)	0.079(3)	0.095(2)	0.0023(2)
CrO ₂ rutile	0.065(2)	0.073(2)	0.076(2)	0.0015(1)	0.074(4)	0.076(4)	0.089(4)	0.0021(3)
V _{0.976} Cr _{0.024} O ₂ monoclinic	0.064(1)	0.080(1)	0.080(2)	0.0017(1)	0.048(8)	0.066(4)	0.081(4)	0.0011(3)
	0.062(1)	0.067(2)	0.081(2)	0.0014(1)	0.053(12)	0.065(6)	0.084(5)	0.0012(5)
VO ₂ monoclinic	0.0010	0.0015
	0.0017

patible with a phonon instability of the same optical mode as that for the insulating phase of VO₂.²⁰

The thermal parameters obtained in the x-ray experiments can also be compared with heat-capacity data if both sets of data are converted to effective Debye temperatures as shown in Fig. 3. This is an extremely simplified model as everything is lumped into one average parameter but such a comparison does suggest the existence of some fairly low-lying vibrational modes in metallic VO₂. The Debye temperatures for TiO₂²¹ and V_{0.86}W_{0.14}O₂⁷ in the rutile phase and VO₂²² in the M₁ phase were calculated from heat-capacity data. The thermal displacements observed in x-ray measurements are a different average over the phonon spectrum than that observed in heat-capacity ex-

periments so that the resulting Θ_D will not be the same.²³ The heat capacity is given by

$$c_v = k \int \frac{x^2 e^x}{(e^x - 1)^2} F(\nu) d\nu / \int F(\nu) d\nu,$$

where $F(\nu)$ is the phonon density of states and $x \equiv h\nu/kT$ ²³; whereas, for a cubic crystal the average over the thermal displacements is

$$\frac{4\pi^2}{3} \sum_k m_k (\bar{u}_{kx}^2 + \bar{u}_{ky}^2 + \bar{u}_{kz}^2) = h \int \left(\frac{1}{2} + \frac{1}{e^x - 1} \right) \nu^{-1} F(\nu) d\nu / \int F(\nu) d\nu,$$

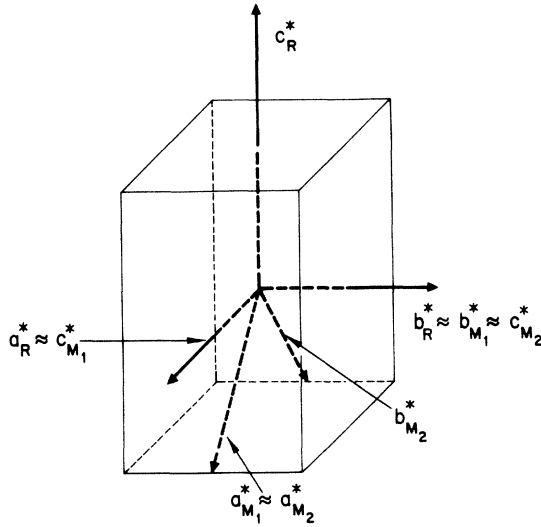


FIG. 2. Diagram showing the relation between reciprocal lattices of R, M₁, and M₂. The Brillouin zone for the rutile phase is outlined to show that $a_{M_1}^*$, $a_{M_2}^*$, and $b_{M_2}^*$ are compatible with a soft zone-edge phonon at $(\frac{1}{2}0\frac{1}{2})$ in rutile being frozen in at the transition.

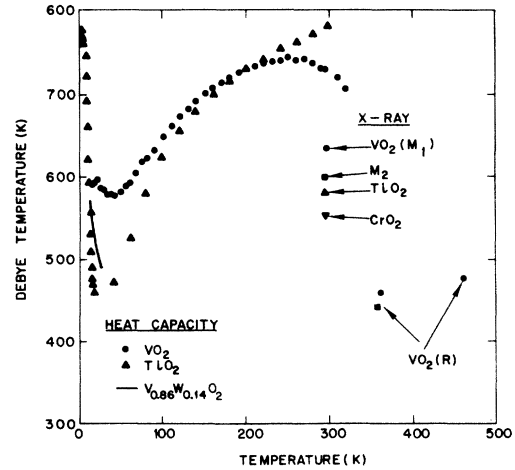


FIG. 3. Comparison of the Debye temperatures obtained from heat capacity and x-ray diffraction measurements. On the left-hand side are heat-capacity results for TiO₂ (triangles), VO₂ (circles) and V_{0.86}W_{0.14}O₂ (solid line) showing the similarity of W doped VO₂ to TiO₂. On the right-hand side are x-ray results at room temperature for VO₂ (M₁—circle), V_{0.976}Cr_{0.024}O₂ (M₂—square), TiO₂ (triangle), and CrO₂ (inverted triangle). These values are substantially higher than those found in the rutile phase of VO₂ (circles at lower right-hand side and V_{0.076}Cr_{0.024}O₂ (square at lower right-hand side).

where the summation is over the k atoms in the unit cell.²³ The correct average for noncubic crystals is not known in simple form; therefore, in order to compare different materials the same average was used for all phases, namely,

$$\bar{u}^2 = \frac{1}{k} \sum_k M_k \bar{u}_k^2,$$

where \bar{u}_k^2 is the average of the k th ellipsoid. The Debye temperatures were then calculated using the standard formula for a monatomic cubic crystal having \bar{u}^2 . In Fig. 3 the values for the rutile phases of TiO₂, VO₂, V_{0.976}Cr_{0.024}O₂, and CrO₂ are given along with those for the M_1 phase of VO₂ and the M_2 phase of V_{0.976}Cr_{0.024}O₂. The large differences in the thermal displacements result in the Debye temperature for metallic VO₂ being 150 °C lower than the other phases shown. The formula above emphasizes that Debye temperatures obtained from x-ray data are heavily weighted on the low-frequency end of the phonon spectrum, thus suggesting some anomalous modes in metallic VO₂. The heat-capacity data support this conclusion as the rutile phase of TiO₂ has a much lower minimum in Debye temperature at low temperatures than does VO₂ which has distorted to the monoclinic phase. The Debye temperature for the metallic rutile phase of V_{0.85}W_{0.14}O₂ is also similar to that of TiO₂ below 40 K. The Debye temperature of VO₂ begins to decrease at ~100 °K below the transition whereas that of TiO₂ continues to rise. This seems too far below the transition to be attributed to stoichiometry effects in a large sample and may reflect precursor effects in the lattice as the metal-insulator transition is approached.

The symmetry of the insulating phases and the large thermal parameters in the metallic phase suggest that the lattice must play an important part in the metal-insulator transition in VO₂. The

evidence for strong electron-electron correlations in the vanadium oxides in general is the large magnetic susceptibility and the large linear term in the heat capacity of the metallic phase at low temperature. In the case of VO₂ the ratio of the effective mass calculated from the susceptibility to that calculated from the optical properties suggests an enhancement in excess of 10. If this represents a spin-fluctuation enhancement in a highly correlated metal, as in the theory of Brinkman and Rice,²⁴ then the mass calculated from the heat capacity at low temperatures would be enhanced by about the same amount. To suppress the insulating phase in order to measure the linear term in the heat capacity of the metallic phase, it was necessary to add 14-mole% WO₂ to VO₂. A large value of γ was found,⁷ but it is questionable if this is representative of the metallic state of pure VO₂, as recent studies have shown that the magnetic susceptibility of the metallic phase increases with increasing concentrations of tungsten.²⁵ In addition large γ 's have been found recently in (Ti_{1-x}V_x)₂O₃ where there is less reason to expect an enhancement due to electron-electron correlations.²⁶ This suggests that electron-electron correlations may be less important in VO₂ than in the lower vanadium oxides such as V₂O₃ and the Magnéli phases. The present work clearly establishes that the thermal factors and the V-V distance along the c axis are anomalous when compared with neighboring phases and other 3d transition metal dioxides, whereas the other V-V distance and the V-O distances are not. It is fair to say that at present none of the existing theories for the metal-insulator transition in VO₂ is compatible with all of the available body of experimental data.

The authors thank T. M. Rice for many stimulating discussions and E. M. Kelly for technical assistance.

*Part of this work done while at Laboratoire de Magnétisme, Centre National de la Recherche Scientifique B. P. 166 38042, Grenoble, France.

†Part of this work done while at Bell Laboratories, Murray Hill, N. J. 07974.

¹T. M. Rice, D. B. McWhan, and W. F. Brinkman, *Proceedings of the Tenth International Conference on the Physics of Semiconductors*, Cambridge, 1970, edited by S. P. Keller, J. C. Hensel, and F. Stein (Natl. Tech. Info. Ser., Springfield, Va., 1970) p. 6293.

²P. Lederer, H. Launois, J. P. Pouget, A. Casalot, and G. Villeneuve, *J. Phys. Chem. Solids* **33**, 1969 (1972).

³N. F. Mott and Z. Zinamon, *Rept. Prog. Phys.* **33**, 881 (1970).

⁴W. Paul, *Mater. Res. Bull.* **5**, 691 (1970).

⁵C. J. Hearn, *Phys. Lett. A* **38**, 447 (1972); *J. Phys. C* **5**, 1317 (1972).

⁶J. B. Goodenough, *J. Solid State Chem.* **3**, 490 (1971).

⁷D. B. McWhan, J. P. Remeika, J. P. Maita, H. Okinaka,

K. Kosuge, and S. Kachi, *Phys. Rev. B* **7**, 326 (1973).

⁸M. Marezio, D. B. McWhan, J. P. Remeika, and P. D. Dernier, *Phys. Rev. B* **5**, 2541 (1972).

⁹D. T. Cromer and J. T. Waber, *Acta Crystallogr.* **18**, 104 (1965).

¹⁰D. T. Cromer, *Acta Crystallogr.* **18**, 17 (1965).

¹¹K. V. K. Rao, S. V. N. Naidu, and L. Iyengar, *J. Phys. Soc. Jap.* **23**, 1380 (1967).

¹²S. C. Abrahams and J. L. Bernstein, *J. Chem. Phys.* **55**, 3206 (1971).

¹³P. Porta, M. Marezio, J. P. Remeika, and P. D. Dernier, *Mater. Res. Bull.* **7**, 157 (1972).

¹⁴C. T. Prewitt, R. D. Shannon, D. B. Rogers, and A. W. Sleight, *Inorg. Chem.* **8**, 1985 (1969).

¹⁵S. Westman, *Acta Chem. Scand.* **15**, 217 (1961).

¹⁶C. J. Hearn, *Solid State Commun.* **12**, 53 (1973).

¹⁷E. Caruthers, L. Kleinman, and H. I. Zhang, *Phys. Rev. B* **7**, 3753 (1973).

¹⁸J. M. Longo and P. Kierkegaard, *Acta Chem. Scand.*

- 24, 420 (1970).
- ¹⁹J. R. Brews, Phys. Rev. B 1, 2557 (1970).
- ²⁰E. I. Blount (private communication).
- ²¹T. R. Sandin and P. H. Keesom, Phys. Rev. 177, 1370 (1969); J. S. Dugdale, J. A. Morrison, and D. Patterson, Proc. R. Soc. A 224, 228 (1954); C. H. Shomate, J. Am. Chem. Soc. 69, 218 (1947).
- ²²E. J. Ryder, F. S. L. Hsu, J. H. Guggenheim, and J. E. Kunzler (unpublished).
- ²³M. Blackman, *Encyclopedia of Physics*, edited by S. Flügge (Springer, Berlin, 1955), Vol. 7, Pt. I.
- ²⁴W. F. Brinkman and T. M. Rice, Phys. Rev. B 2, 4302 (1970).
- ²⁵T. Hörlin, T. Niklewski, and M. Nygren, Mater. Res. Bull. 7, 1515 (1972).
- ²⁶M. E. Sjöstrand and P. H. Keesom, Phys. Rev. B 7, 3558 (1973).